



Exceptional service in the national interest

A numerical study of the length-scale dependence of pool fire behavior using large eddy simulation

Josh McConnell, John Hewson

18th International Conference on Numerical Combustion

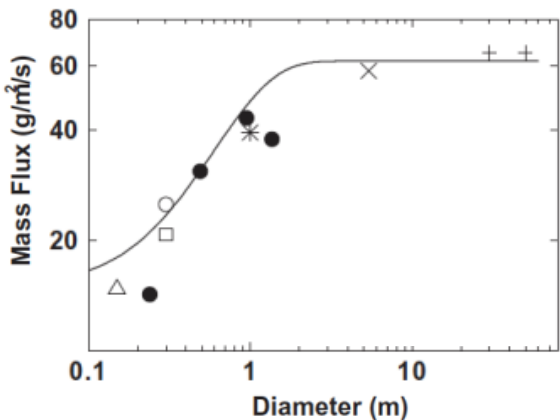
May 9 2022

Sandia National Laboratories is a multimission laboratory managed and operated by National Technology and Engineering Solutions of Sandia LLC, a wholly owned subsidiary of Honeywell International Inc. for the U.S. Department of Energy's National Nuclear Security Administration under contract DE-NA0003525.



Motivation

- Heat flux to the pool surface and vaporization rate is observed to increase for medium diameters and level off for large diameters.
 - This is associated with increasing radiation heat flux followed by optically thick conditions where radiative flux to the pool surface is constant W.R.T. pool diameter.
- Experimentally studying the how flame interior radiative heat transfer evolves with changing pool diameter is difficult for large sooting flames.





Model formulation: governing equations

continuity

$$\int \frac{\partial \bar{\rho}}{\partial t} dV + \int \bar{\rho} \tilde{u}_j n_j dS = - \int \textcolor{blue}{S_{Y_{soot}}} dV$$

momentum

$$\int \frac{\partial \bar{\rho} \tilde{u}_i}{\partial t} dV + \int \bar{\rho} \tilde{u}_i \tilde{u}_j n_j dS = \int \left(\tilde{\sigma}_{ij} - \tau_{ij}^{sgs} \right) n_j dS + \int (\bar{\rho} - \rho_{\circ}) g_i dV$$

Mixture fraction

$$\int \frac{\partial \bar{\rho} \tilde{Z}}{\partial t} dV + \int \bar{\rho} \tilde{u}_j \tilde{Z} n_j dS = \int \left(\frac{\bar{\mu}}{Sc} \frac{\partial \tilde{Z}}{\partial x_j} - \tau_{Z,j}^{sgs} \right) n_j dS - \int \textcolor{blue}{S_{Y_{soot}}} dV$$

enthalpy

$$\int \frac{\partial \bar{\rho} \tilde{h}}{\partial t} dV + \int \bar{\rho} \tilde{u}_j \tilde{h} n_j dS = \int \left(\frac{\bar{\mu}}{Pr} \frac{\partial \tilde{h}}{\partial x_j} - \tau_{h,j}^{sgs} \right) n_j dS - \int \textcolor{red}{S_h} dV$$

Soot mass

$$\int \frac{\partial \bar{\rho} \tilde{Y}_{soot}}{\partial t} dV + \int \bar{\rho} \tilde{u}_j \tilde{Y}_{soot} n_j dS = \int \left(\frac{\bar{\mu}}{Pr} \frac{\partial \tilde{Y}_{soot}}{\partial x_j} - \tau_{Y_{soot},j}^{sgs} \right) n_j dS + \int \textcolor{blue}{S_{Y_{soot}}} dV$$

Soot particle concentration

$$\int \frac{\partial \bar{\rho} \tilde{N}_{soot}}{\partial t} dV + \int \bar{\rho} \tilde{u}_j \tilde{N}_{soot} n_j dS = \int \left(\frac{\bar{\mu}}{Pr} \frac{\partial \tilde{N}_{soot}}{\partial x_j} - \tau_{N_{soot},j}^{sgs} \right) n_j dS + \int \textcolor{green}{S_{N_{soot}}} dV$$

- The enthalpy source term, $\textcolor{red}{S_h}$, includes radiative terms from gas and soot.
- Source terms for soot mass and particle concentration have the following form:

$$\textcolor{brown}{S_{N_{soot}}} = S_{\text{nucleation}} - S_{\text{coagulation}} \tilde{Y}_{soot}^{1/6} \tilde{N}_{soot}^{11/6}$$

$$\textcolor{blue}{S_{Y_{soot}}} = W_{\text{soot}} S_{\text{nucleation}}$$

$$+ [S_{\text{surface growth}} - S_{\text{ox,O}_2} - S_{\text{ox,O}_H}] \tilde{Y}_{soot}^{2/3} \tilde{N}_{soot}^{1/3}$$

- $S_{\text{nucleation}}$, $S_{\text{coagulation}}$, etc. are computed based on the Aksit-Moss soot model.
- These terms depend on a number of species concentrations which are computed from a flamelet model.

Model formulation: Flamelet equations

- flamelet equation solution parametrizes $\phi = \{Y_i, T\}$ in terms of 3 variables:

$$\phi = \phi(Z, \chi, \gamma)$$

$$\chi = 2D_Z |\nabla Z|^2$$

$$\gamma = h - h_c$$

- Convolution of ϕ with a presumed PDF provides an interface between filtered values of Z, χ, γ and flamelet solutions.

$$\frac{\partial Y_i}{\partial t} = \frac{\chi}{2} \frac{\partial^2 Y_i}{\partial Z^2} + \frac{\omega_i}{\rho}$$

$$\frac{\partial T}{\partial t} = -\frac{1}{\rho c_p} \sum_{i=1}^{n_s} \omega_i h_i - \left(\frac{\partial^2 T}{\partial Z^2} + \frac{\partial T}{\partial Z} \frac{\partial c_p}{\partial Z} + \frac{\partial T}{\partial Z} \sum_{i=1}^{n_s} \frac{c_{p,i}}{c_p} \frac{\partial Y_i}{\partial Z} \right) + S_T(Z, T, \chi)$$

Implicitly depends on γ

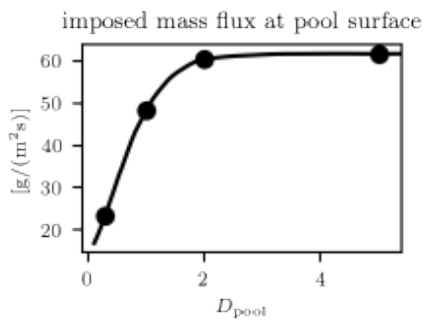
Scalar variance:
determined from
turbulence model

Presumed mixture
fraction PDF

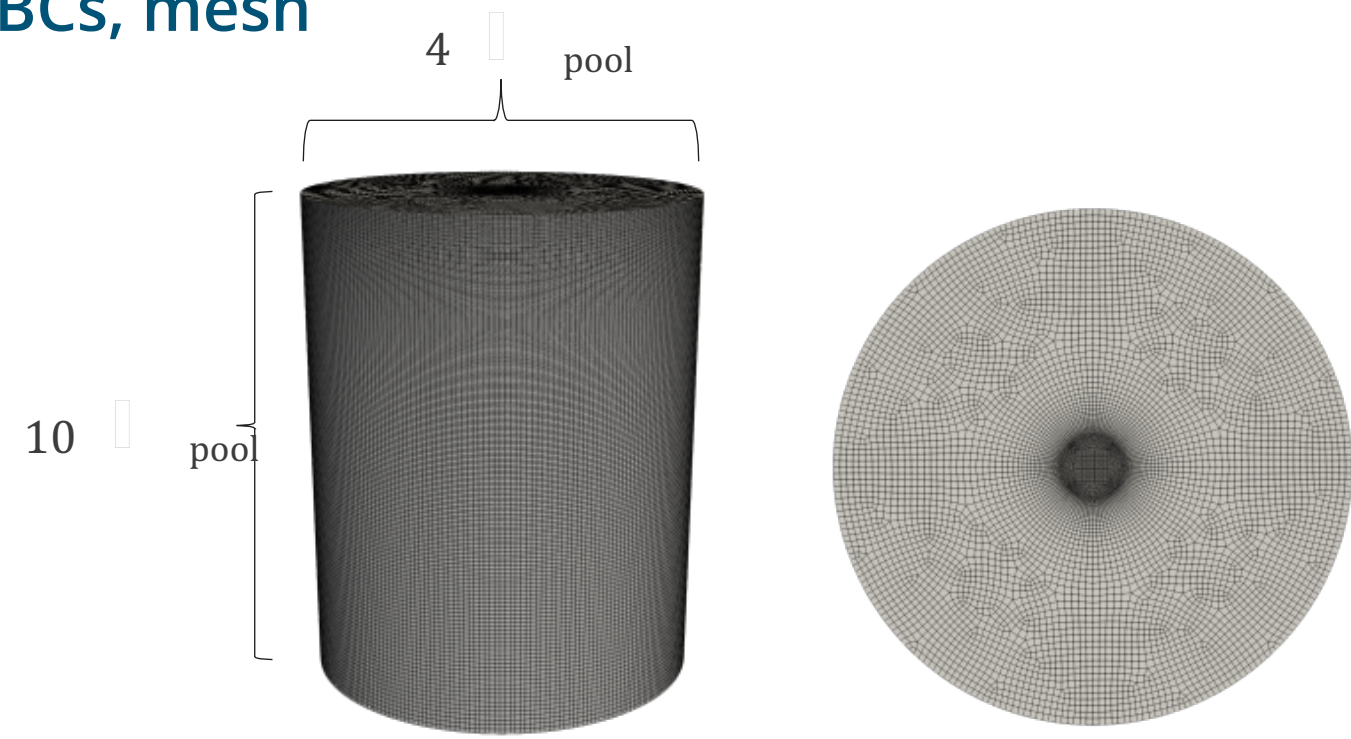
$$\tilde{\phi}(\tilde{Z}, \tilde{Z}'^2, \tilde{\chi}, \tilde{\gamma}) = \int_0^1 \phi(Z, \chi, \gamma) P_Z(Z | \tilde{Z}, \tilde{Z}'^2) dZ, \tilde{\gamma} = \gamma, \tilde{\chi} = \chi$$

Computational setup; ICs, BCs, mesh

- 4 pool fire diameters considered: 0.3, 1, 2, and 5 meters.
- Cylindrical Domain:
 - 4 pool diameters wide
 - 10 pool diameters high
- BCs at pool surface:
 - $T_{pool} = 300$ K
 - Mass flux set based on empirical correlation (Ditch *et al.* [1]).



- Domain initially consists of air ($Z = 0$) at 300 K.

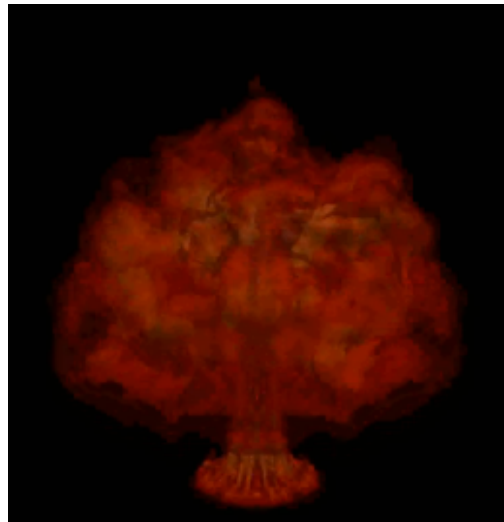


	0.3 m	1 m	2 m	5 m
Pool mass flux $[g/m^2s]$	23.46	48.15	60.35	61.64
Mesh resolution	0.3 cm	1 cm	2 cm	2.5 cm

Results

- Animation playback speed is scaled by $D_{\text{pool}}^{1/2}$.
- Calculations for each pool size are run out for at least 10 puff cycles.

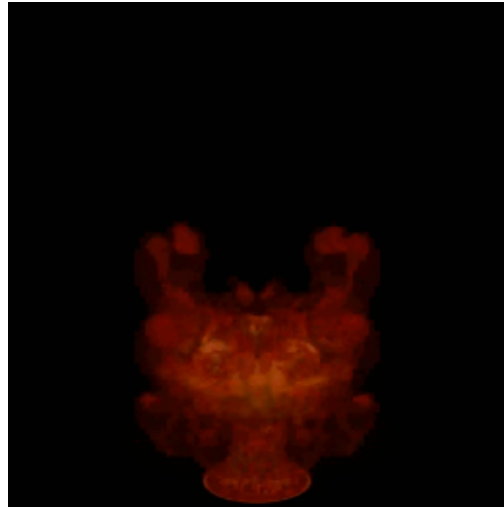
pool = 0.3 m



pool = 1 m



pool = 2 m

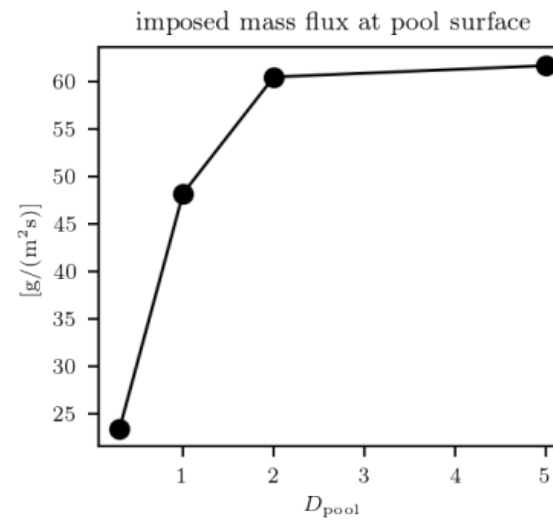


pool = 5 m



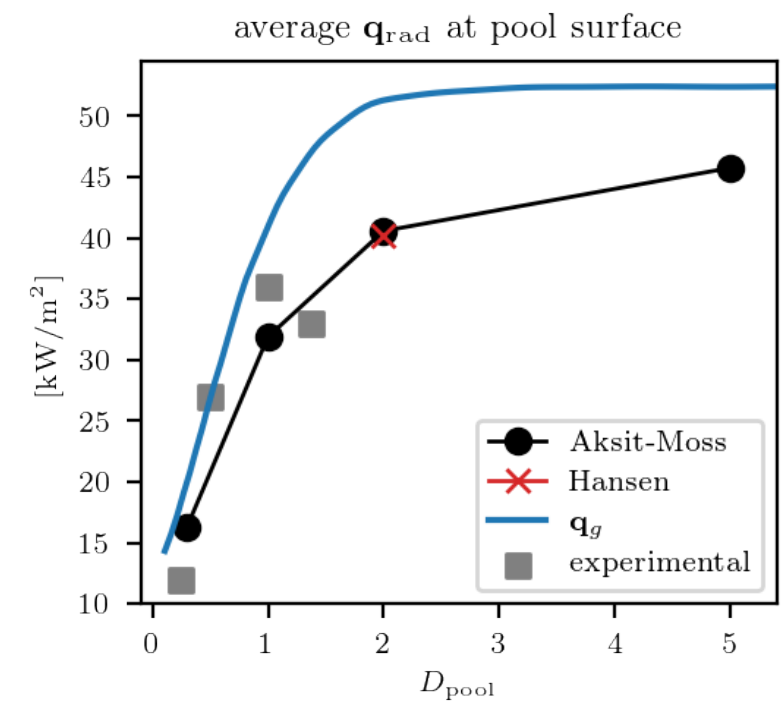
Radiative heat fluxes at pool surface

- Computed radiative heat fluxes agree with measured values .
- Discrepancy between \mathbf{q}_{rad} and \mathbf{q}_g due to
 - Decoupled \mathbf{q}_{rad} and \dot{N}_{pool} .
 - Non-negligible convective heat flux for small D_{pool} .



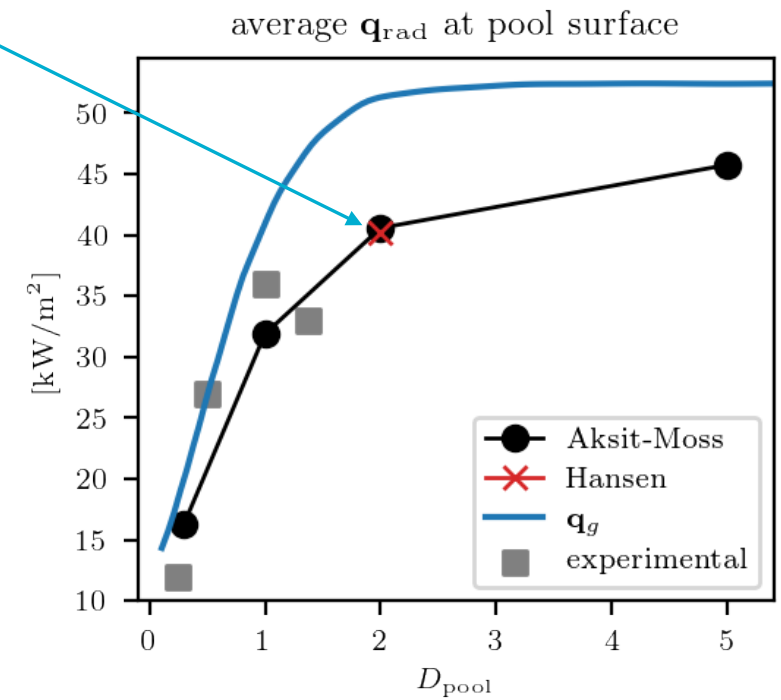
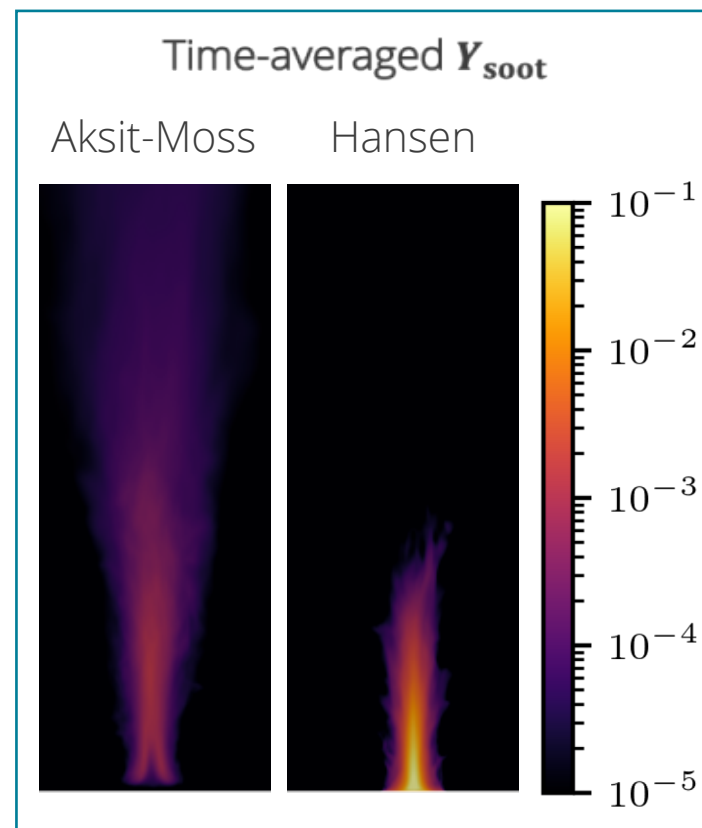
$$\mathbf{q}_g = \dot{N}_{\text{pool}} \Delta h_g$$

$$\Delta h_g = L_v(T_b) + \int_{T_0}^{T_b} C_p(T) dT$$

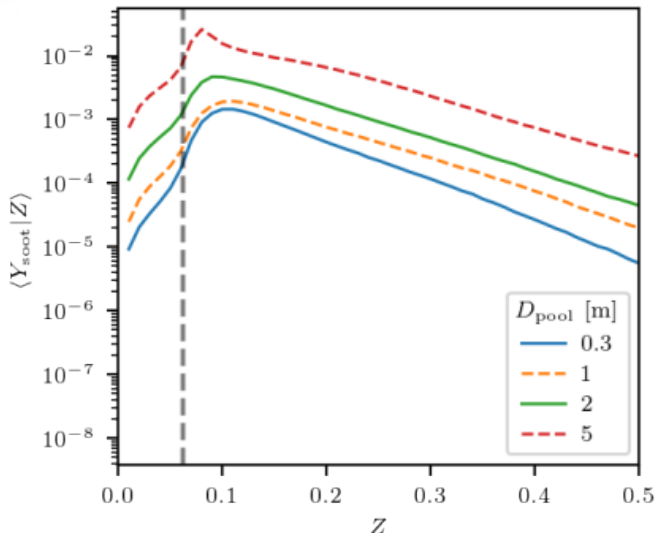


Radiative heat fluxes at pool surface

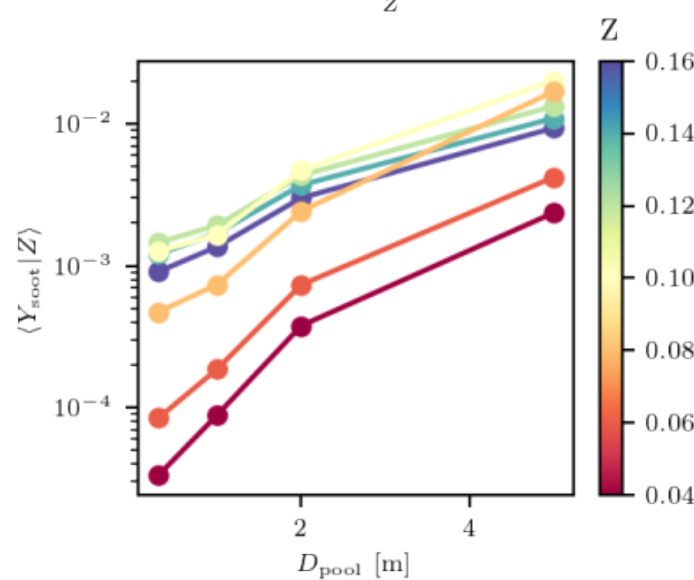
- Comparison of simulations using different soot models indicate q_{rad} at pool surface is insensitive to Y_{soot} if Y_{soot} is sufficiently large.



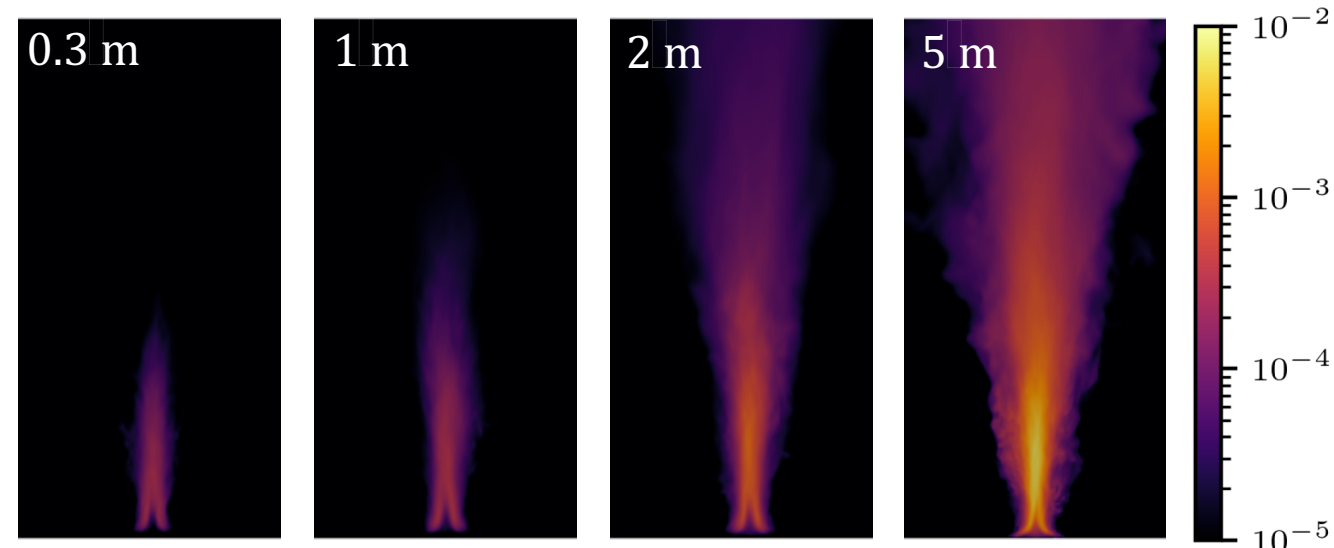
Soot concentration dependence on D_{pool}



- Trends of $\langle Y_{\text{soot}} | Z \rangle$ reflect those for time-averaged Y_{soot} .
- For fixed Z , computed $\langle Y_{\text{soot}} | Z \rangle$ grows approximately exponentially W.R.T D_{pool} for $D_{\text{pool}} \leq 2$ m.
 - This behavior should become asymptotic for sufficiently large D_{pool} .

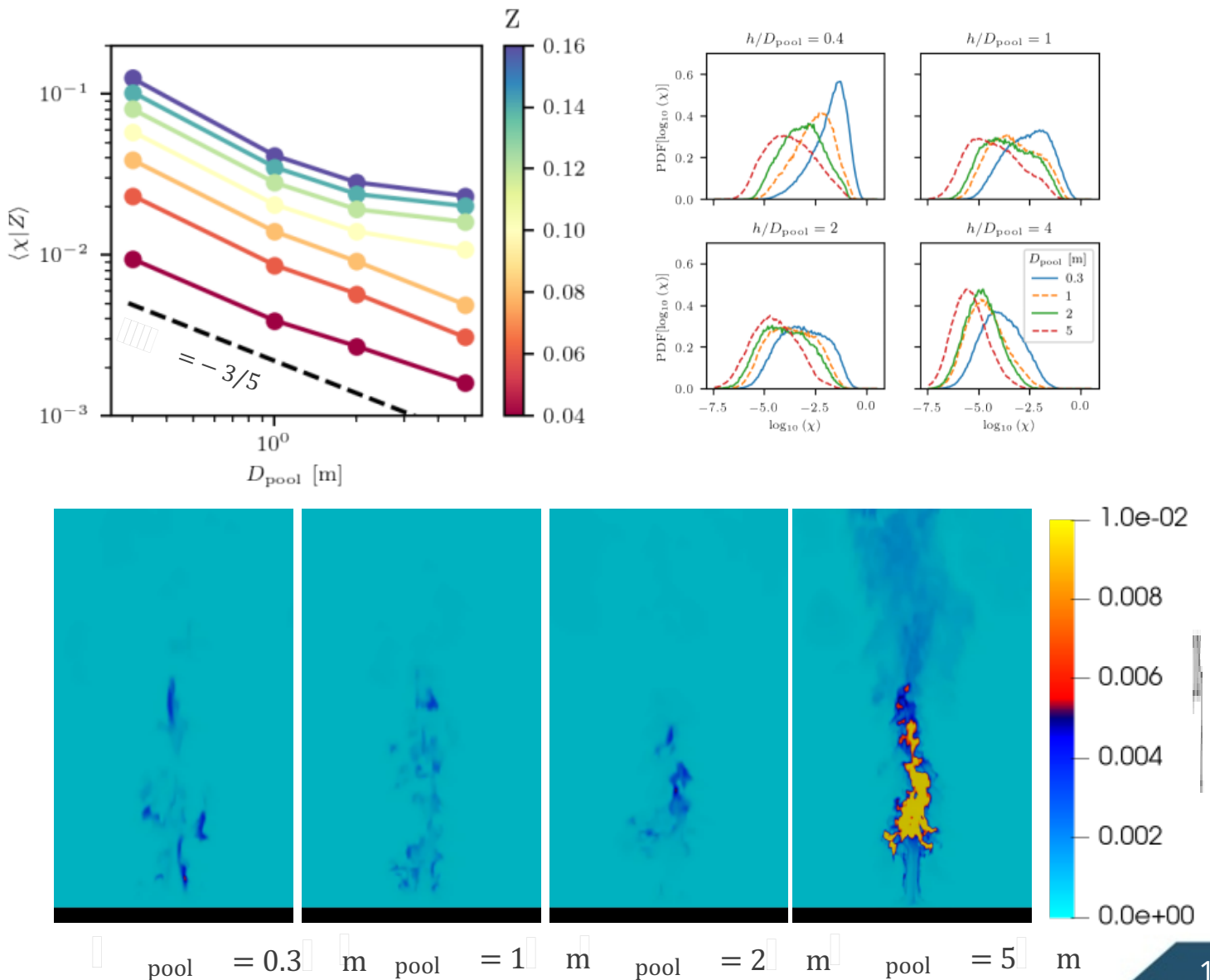


Time averaged Y_{soot}



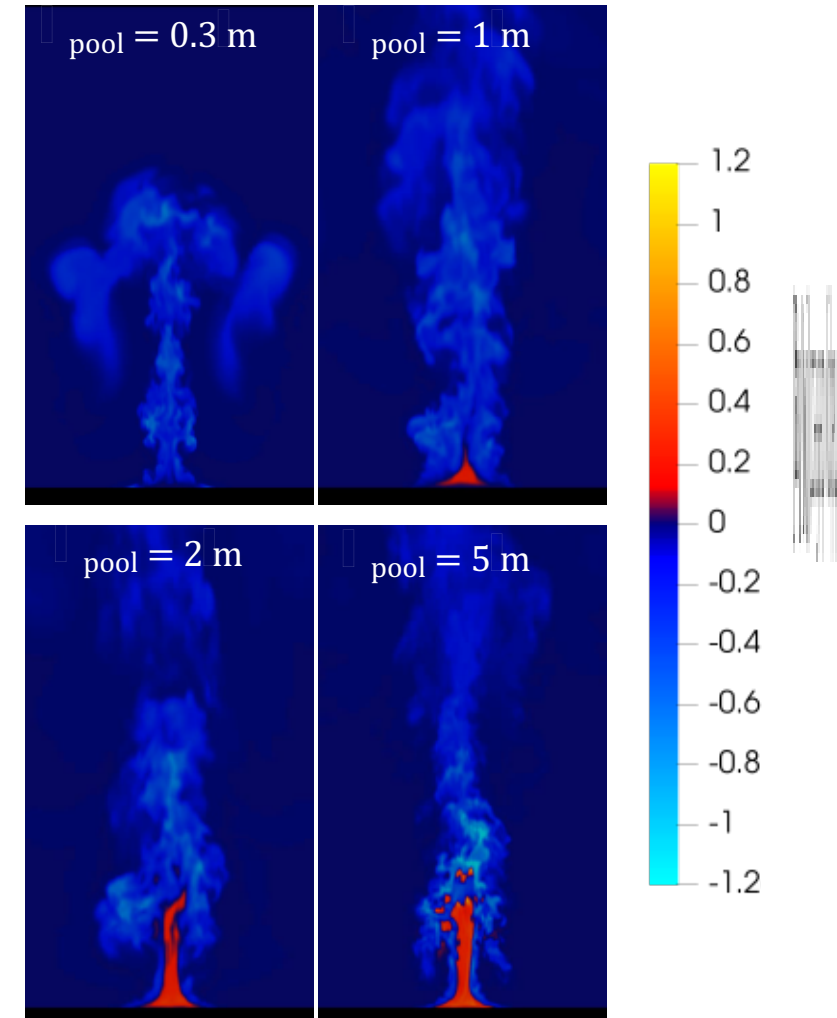
Small-scale mixing dependence on D_{pool}

- Scalar dissipation rate decreases with increasing D_{pool}
 - What this indicates:
As D_{pool} is increased, the proportion of the volume that scalar gradients are created is reduced with increasing D_{pool} .
 - This results in large, fuel-rich regions where soot formation is controlled by reaction kinetics for large enough D_{pool} .

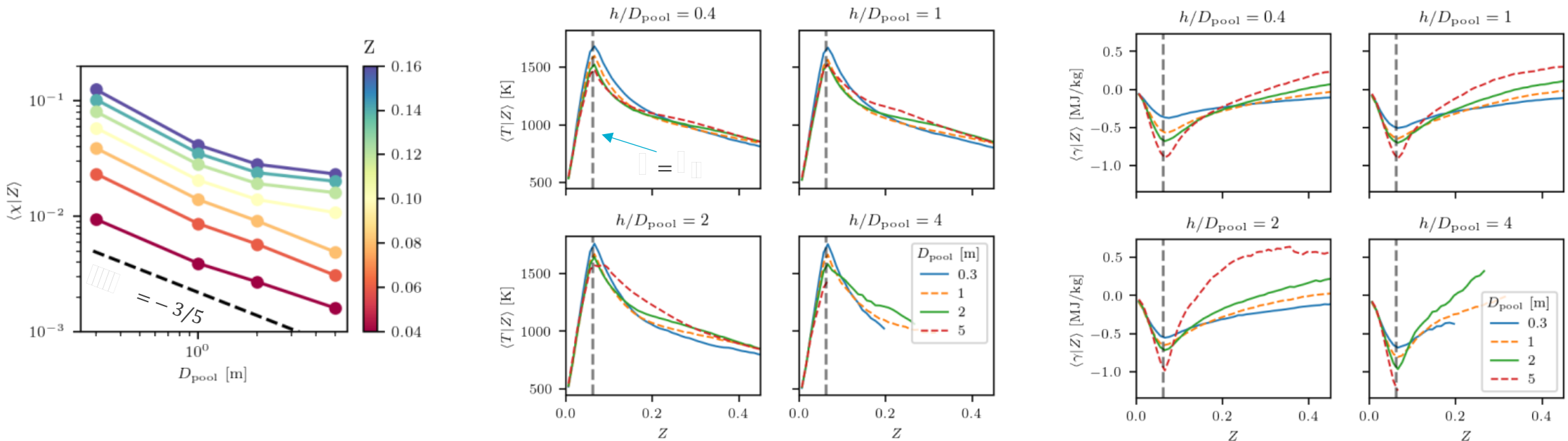


Magnitude of enthalpy defect grows with D_{pool}

- Enthalpy defect = $h - h_{ad}$.
- Sufficiently-large fires exhibit super-adiabatic regions.
 - These regions appear within the interior of the fire.
 - If the fire is large enough, transient superadiabatic regions appear in the upper portion of the flame.

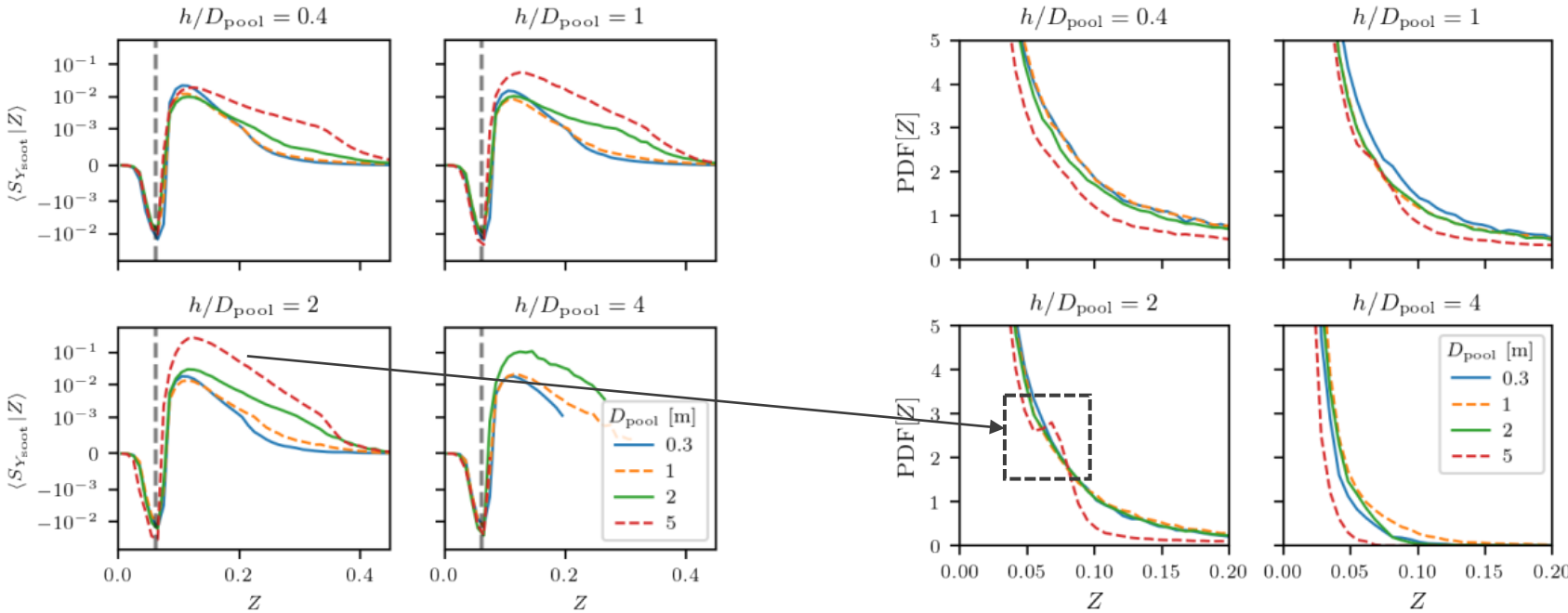


Magnitude of enthalpy defect grows with D_{pool}



- As D_{pool} increases, χ decreases \rightarrow slower mixing .
- *Consequently,*
 - Lifetime of fuel-rich regions increases allowing for more soot formation
 - Radiation distributes energy from hot regions ($Z \approx Z_{st}$) to cooler sooty, fuel-rich regions.
 - Less mixing of super- and subadiabatic regions.

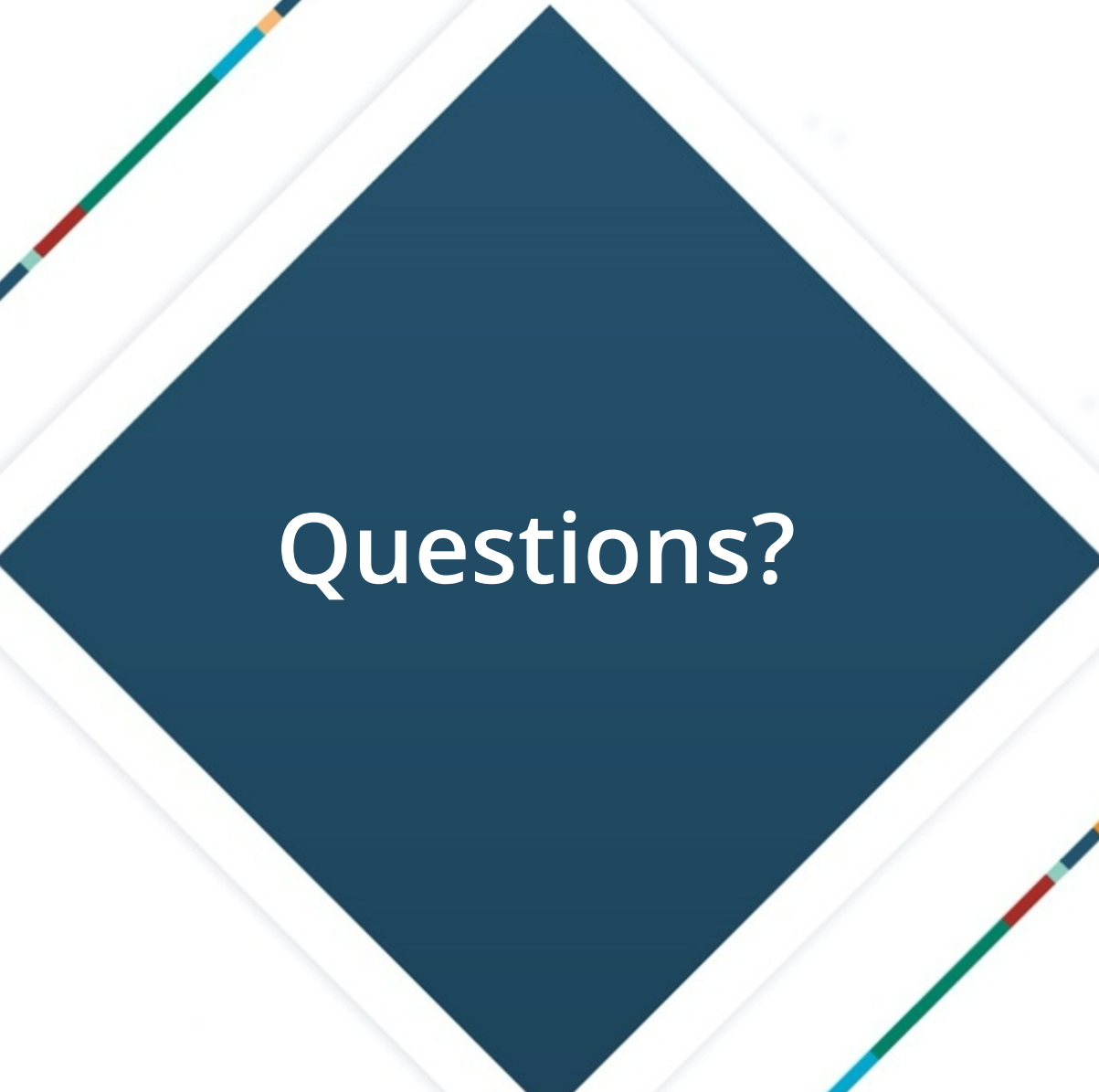
Behavior of mixture fraction distribution



- $PDF[Z]$ shifts towards lower values of Z as D_{pool} increases
 - This occurs because total soot production increases W.R.T D_{pool}
- Local max. in $PDF[Z]$ occurs for $D_{pool} = 5$ m over a certain range of heights.
 - under rich conditions ($Z > Z_{st}$) soot formation dominates soot oxidation, so a net removal of gaseous fuel occurs which decreases Z , and
 - for lean conditions ($Z < Z_{st}$), soot oxidation is dominant so that mass originating from the fuel is readded to the gas phase which increases Z .

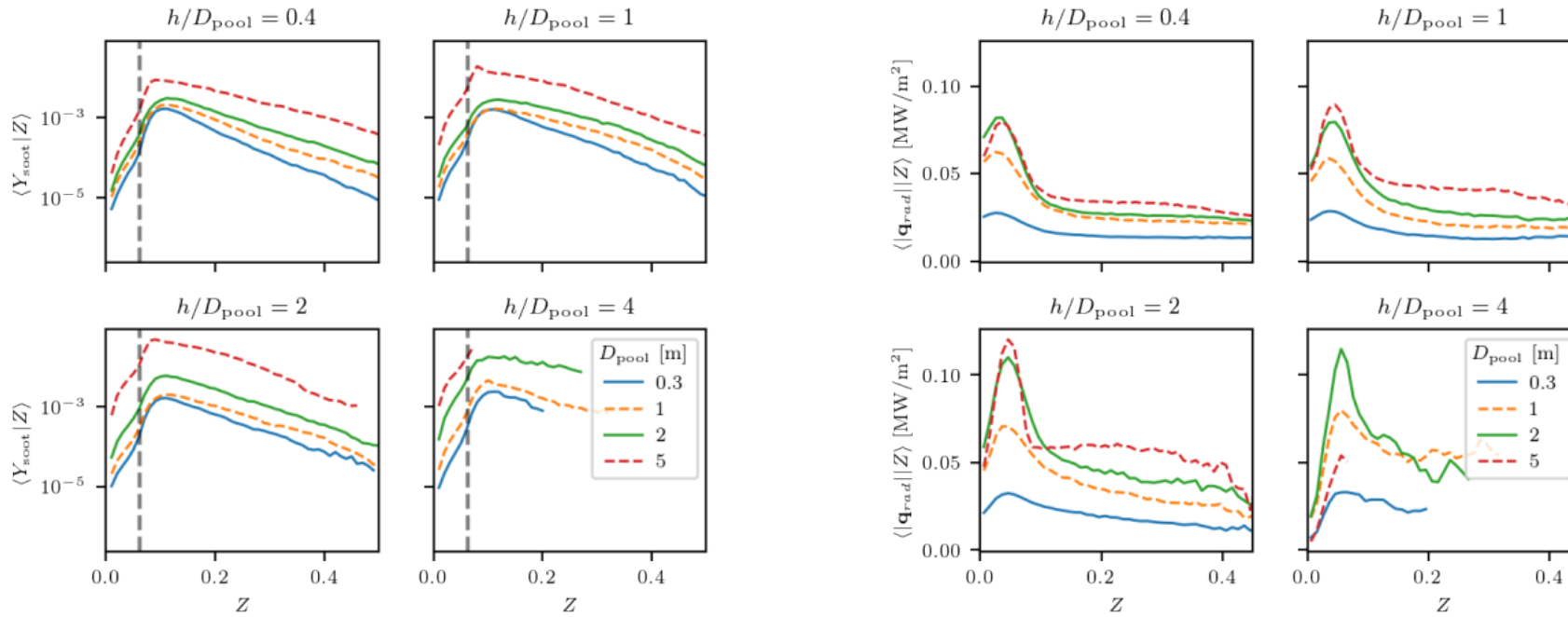


Summary and conclusions

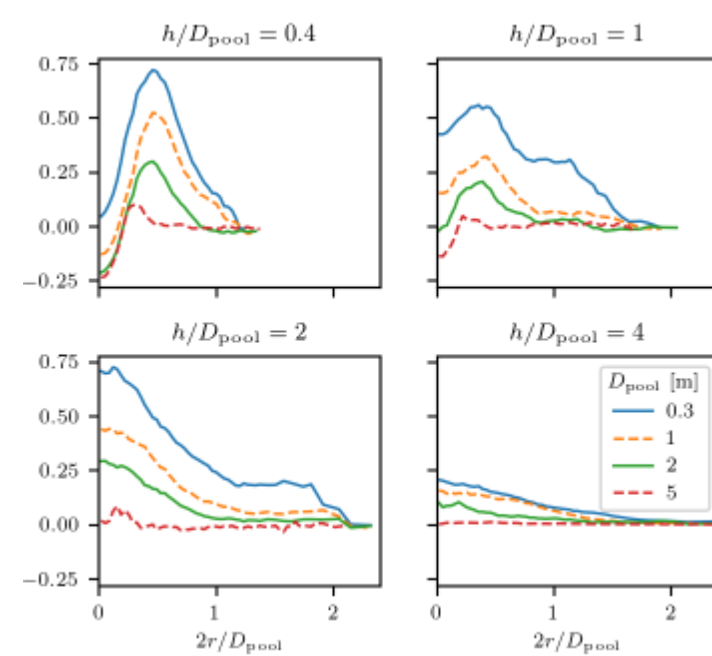
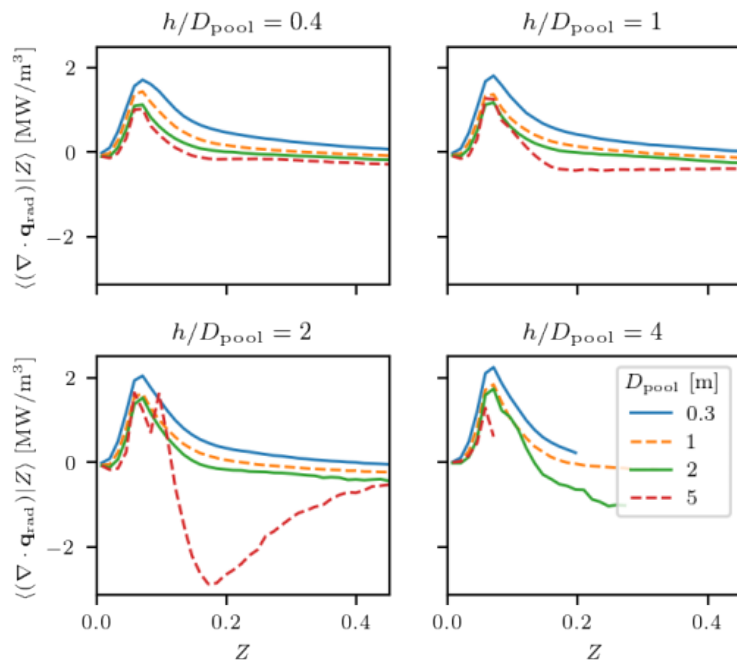


Questions?

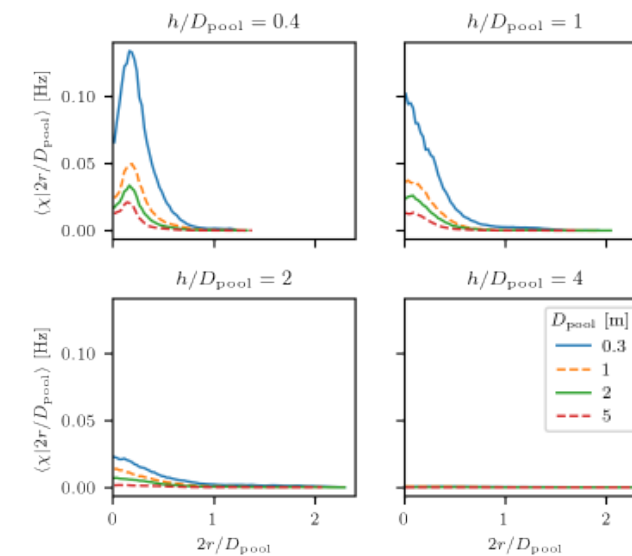
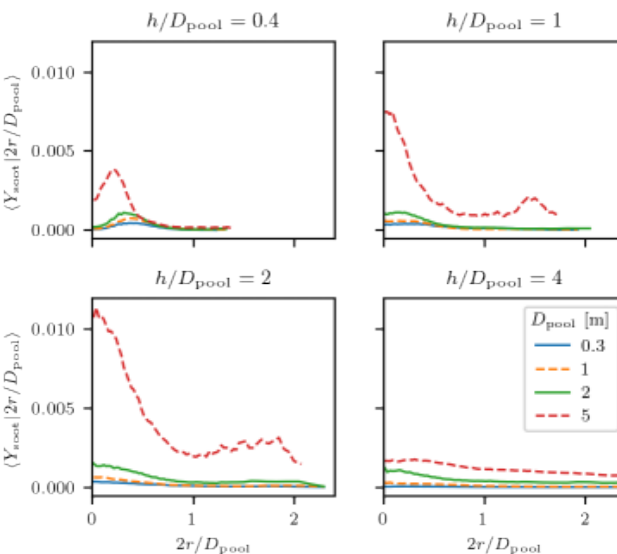
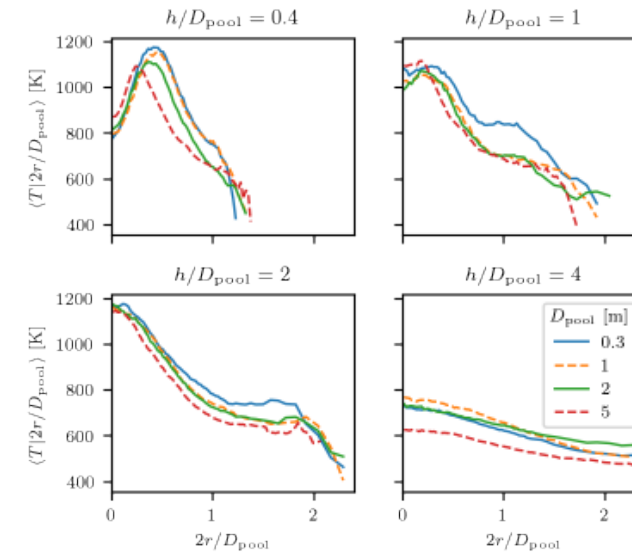
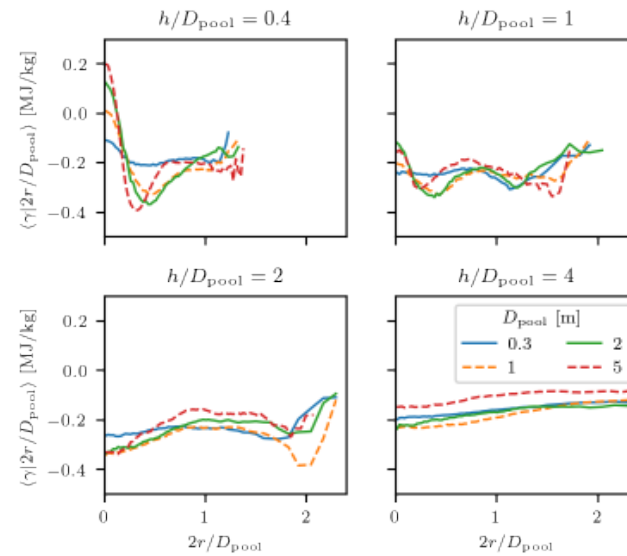
Soot concentration and radiative heat flux heat flux vs. mixture fraction



Divergence of radiative heat flux



Enthalpy defect, temperature, soot concentration, and scalar dissipation rate

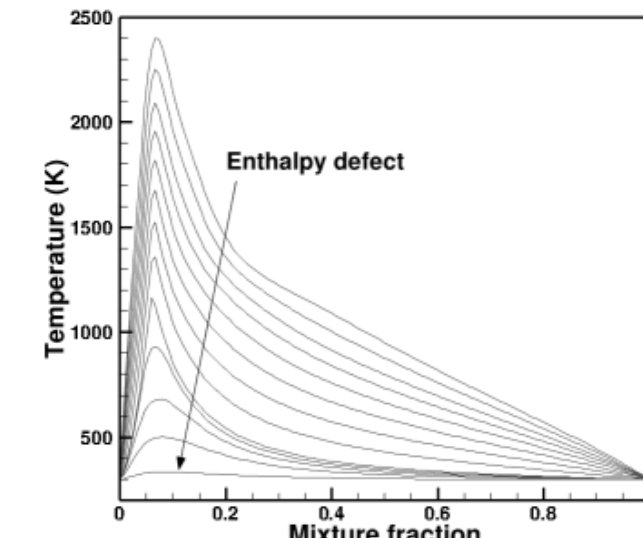
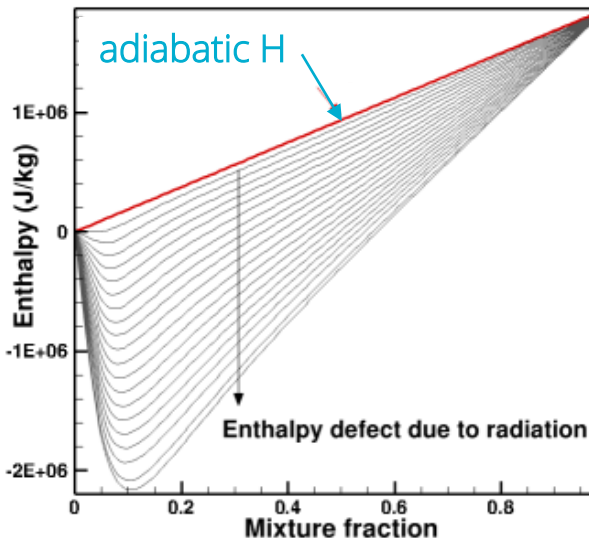
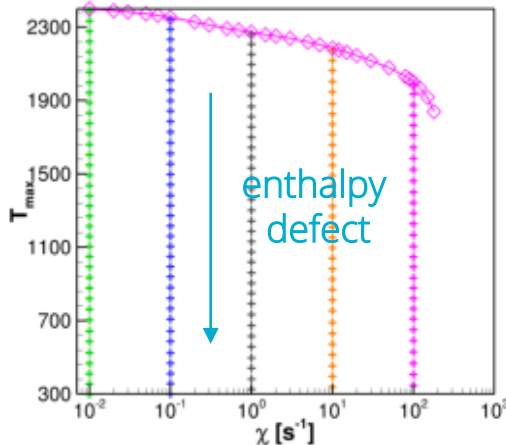


Non-Adiabatic Flamelets

- To allow for radiative quenching and generalize to other heat losses, a new heat-loss term is proposed:
 - Proportional to χ for complete cooling $\frac{\partial H}{\partial t} + \frac{\chi}{2} \frac{\partial^2 H}{\partial Z^2} = h_0 \chi \left[\frac{T(H, Z) - T_\infty}{T_{max} - T_\infty} \right]$
 - Linear in temperature: better off-stoich coverage
- With the larger sink term, flame cools down to ambient T
 - This is 'cooled product', not reactants mixing
- Enthalpy defect $\tilde{\gamma}$ is introduced

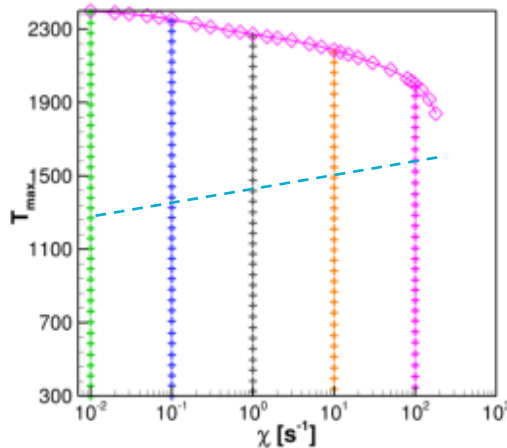
$$\tilde{\gamma} = \tilde{H} - \widetilde{H}_{ad}$$

$$\widetilde{H}_{ad} = H(0) + [H(1) - H(0)] \tilde{Z}$$

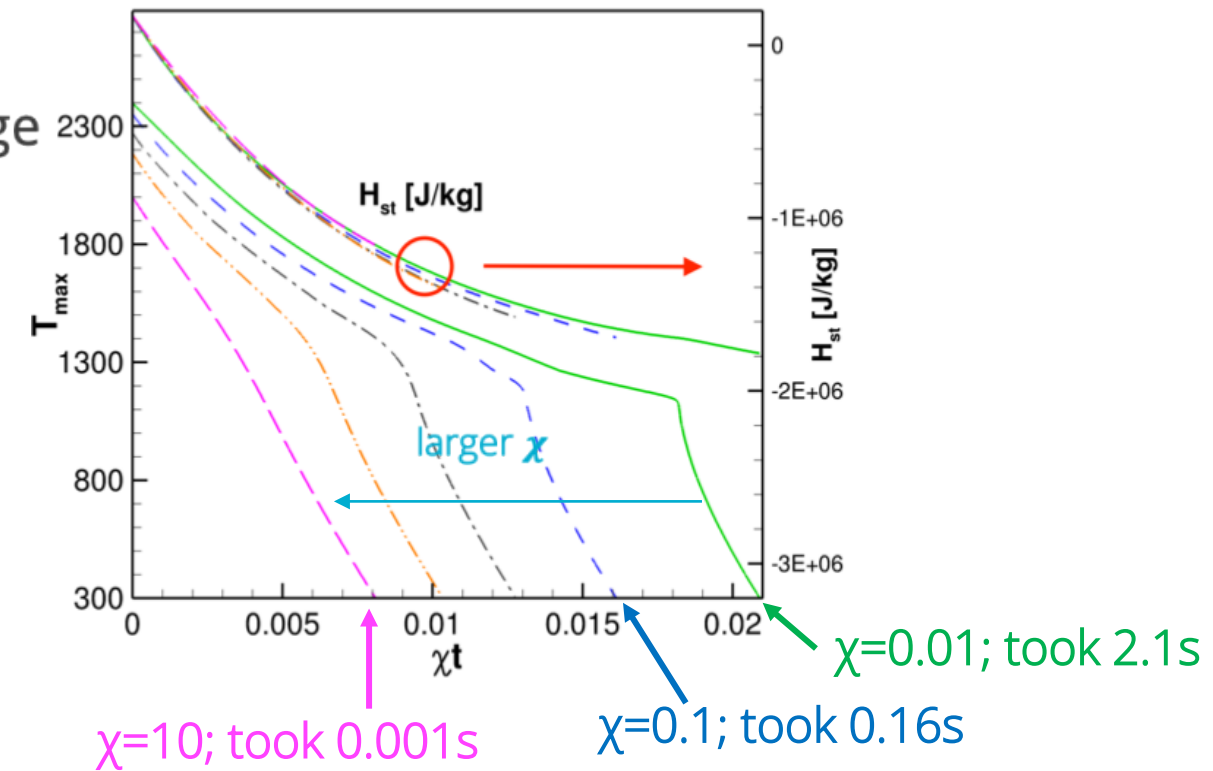


Unsteady flamelet cooling

- **Heat loss and heat release both scale by χ .**
- Normalize by $(T_{max} - T_0)$ to retain the same magnitude with time.
- Timescale matches estimated enthalpy response time
- $O(0.1\text{-}1\text{s})$ for complete cooling at lower χ range
- Max temp falls faster below unstable middle branch.



$$\frac{\partial H}{\partial t} + \frac{\chi}{2} \frac{\partial^2 H}{\partial Z^2} = h_0 \chi \left[\frac{T(H, Z) - T_\infty}{T_{max} - T_\infty} \right]$$

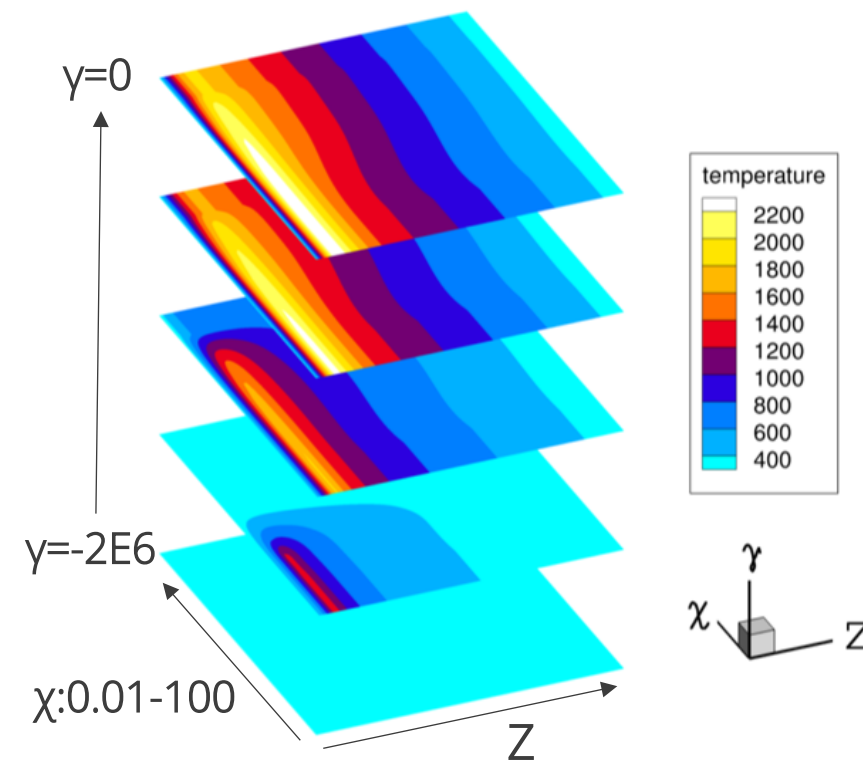
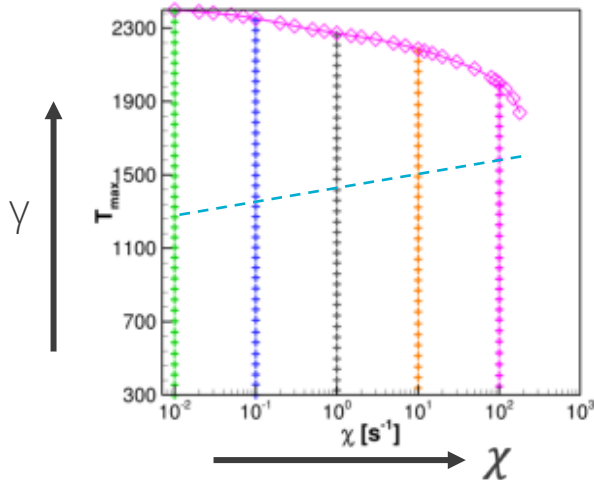


Tabulation

- Tabulation of χ -based enthalpy defect approach is preferred for fire and similar scenarios over progress variable approach.
 - Progress variable predicts ignition delay, local quenching/re-ignition for fast mixing.
 - No heat losses are associated with progress variable decrement.
 - χ is orthogonal to γ .

Sub-filter PDF applied to the mixture fraction: results in 4-d table

\tilde{Z} , $\widetilde{Z''^2}$, $\tilde{\chi}$, and $\tilde{\gamma}$



Tabulation – orthogonal transformation

To generate structured table, presumed form of $\gamma(Z)$: $\gamma = \gamma_o F_\gamma(Z, Z_o) = \begin{cases} \frac{Z}{Z_o} & : Z \leq Z_o \\ \frac{1-Z}{1-Z_o} & : Z > Z_o \end{cases}$

- Extract table location from convolved form, F .
- Store results in B-splines.
- Logarithmic spacing for \tilde{Z}''^2

$$\gamma_0 = \frac{\tilde{\gamma}}{\int_0^1 F_\gamma(Z, Z_0) p_Z(\tilde{Z}, \tilde{Z}''^2) dZ}$$

